Paper-ID: VGI_199627

SAR Interferometry: Experiences with ERS-1/2 SLC Data

Lado Kenyi [1], Johannes Raggam [2], Mathias Schardt [3]

[1] *Institute for Digital Image Processing, Joanneum Research, Wastiangasse 6, A-8010 Graz*
[2] *Institute for Digital Image Processing, Joanneum Research, Wastiangasse 6, A-8010 Graz*
[3] *Institute for Digital Image Processing, Joanneum Research, Wastiangasse 6, A-8010 Graz*

VGI – Österreichische Zeitschrift für Vermessung und Geoinformation **84** (2), S. 157–164

1996

BibTEX:

```
@ARTICLE{Kenyi_VGI_199627,
Title =  {SAR Interferometry: Experiences with ERS-1/2 SLC Data},
Author =  {Kenyi, Lado and Raggam, Johannes and Schardt, Mathias},
Journal =  {VGI -- {\"O}sterreichische Zeitschrift f{\"u}r Vermessung und
   Geoinformation},
Pages =  {157--164},
Number =  {2},
Year =  {1996},
Volume =  {84}
}
```



SAR Interferometry: Experiences with ERS-1/2 SLC Data

Lado Kenyi, Hannes Raggam and Mathias Schardt, Graz

Zusammenfassung

Es wird ein allgemeiner Überblick über die Verarbeitung von interferometrischen SAR (INSAR) Daten, welche von den ERS Sensoren aufgenommen werden, gegeben. Die einzelnen Schritte der implementierten Verarbeitungskette werden mittels bildhaften Zwischenprodukten illustriert. Für 3 Testgebiete wurden mittels der INSAR Technologie digitale Höhenmodelle erstellt und diese interferometrisch hergeleiteten DHMs im Vergleich zu bestehenden Referenzmodellen analysiert. Es wird gezeigt, daß mittels INSAR erstellte DHMs eine hohe Qualität haben können, falls die Kohärenzen der verwendeten Datensätze auch ausreichend hoch sind. Weiters wird demonstriert, daß neben reduzierter Kohärenz auch atmosphärische Turbulenzen einen beachtlichen Fehlereinfluß auf die INSAR Höhenmessungen haben können.

Abstract

A general overview on the processing of interferometric SAR (INSAR) data acquired by the ERS sensors is given. The individual steps of the implemented processing chain are illustrated by intermediate image products. For 3 test areas digital elevation models were produced using the INSAR tools and a comparative analysis of these interferometrically derived DEMs is given with respect to existing reference DEMs. It is shown that INSAR derived elevation models may show a high quality when the coherency in the data sets being used is sufficiently high. It is also demonstrated that beside reduced coherency, atmospheric turbulence can induce significant errors in the INSAR height measurements.

1. Introduction

A regular SAR system maps the earth's surface into a two-dimensional SAR image. The individual resolution cells are represented in a two-dimensional matrix of pixels with the brightness being proportional to the power of the SAR echo. The line of the pixel matrix corresponds with the along track position of the SAR during the imaging procedure, and the column identifies the slant range of the resolution element with respect to the SAR sensor. The interferometric synthetic aperture radar technique or INSAR introduces a further step which is the provision of additional information about the third dimension of the resolution cell's position by a signal correlation method applied on a pixel-by-pixel basis to two SAR images representing the same scene. The two SAR images can be acquired either simultaneously in a single pass by two antennas, or at different positions at different times in multiple passes by a single antenna. The power measured is focused and correlated to a complex pixel value, with the in-phase component representing the real part and the quadrature component the imaginary part. Hence, such data are supplied as single look complex (SLC) images. Using the INSAR processing technique it is possible to produce detailed and accurate three dimensional relief maps of the earth's surface directly from the SLC data [6, 10]. The technique can also be used to detect very small movements of land surface features in the cm-range which is known as differential interferometry [1, 5, 9].

Until now, ERS INSAR data have been acquired either by ERS-1 in time intervals of 3 or 35 days – or multiples therefrom – between the image pairs, or recently by a combination of an ERS-1 and an ERS-2 SLC scene being acquired during the ERS Tandem mission. This mission was specifically designed for the acquisition of appropriate SLC image pairs within a period of typically one day, which is the repeat orbit interval between ERS-1 and ERS-2.

The Institute for Digital Image Processing of Joanneum Research has been actively involved in the field of geometric treatment of SAR image products. The results of this long term experience have been manifested in the Remote Sensing Software Graz (RSG). As an upgrade of the RSG and to cope up with the new developments in the field of SAR remote sensing, modules or tools for the processing of INSAR data have been developed and added to the RSG. In this paper, we present results of experiments in generating INSAR products, especially DEMs from

ERS-1/2 SLC data. The presentation includes the interferometric processing chain up to phase unwrapping, the generation of DEMs, the discussion of the results obtained and concluding remarks.

2. Test Area and SLC Data

In general, experiments made over 3 different test sites are presented in this paper. These are:

Test area „Bonn":

For the area west of the city of Bonn in Germany SLC data acquired by ERS-1 in a 15 days time interval were analysed with regard to an investigation for the detection and interpretation of atmospheric effects on interferometric data [4].

Orbits: 03459 and 03674
Dates: 14-03-1992 and 29-03-1992
Baseline: 156 meters

Test area „Dortmund":

For an area south-west of the city of Dortmund in Germany, the following ERS-1 SLC image pair was processed:

Orbits: 12864 and 12907
Dates: 31-12-1993 and 03-01-1994
Baseline: 71 meters

Test area „Graz":

This test site covers the city of Graz as well as the south-western areas and is intended for use in a study concerning temporal decorrelation. An ERS Tandem SLC image pair was used for this area with acquisition dates as follows:

Orbits: 21338 (ERS-1) and 01665 (ERS-2)
Dates: 14-08-1995 and 15-08-1995
Baseline: 56 meters

3. Interferometric Data Processing

In the following, the interferometric processing chain is described up to the phase unwrapping. As an illustration, intermediate products derived from the Dortmund test data are presented.

3.1 Co-registration

The INSAR processing starts with the co-registration of the images to a subpixel accuracy of 1/30. This is achieved by first correlating patches of 25×25 pixels to a pixel accuracy and by a subsequent surface fitting in a 3×3 window around the maximum point in order to obtain the subpixel accuracy. This process is repeated for a number of points covering the whole image, where only those points showing high correlation values are considered. After the offsets determination, one of the images is aligned to the other by polynomial interpolation.

3.2 Interferogram Generation

Next, the co-registered images are cross correlated to generate the interferogram, which is a complex image too. Ideally, the two SLC images should be spectrally shift filtered in the range and spectrally aligned in the azimuth direction to maximise the coherency. The two SLC images should also be over-sampled at least by a factor of two prior to the cross correlation to minimise aliasing. However, the spectral shift filtering is only of significance with SLC image pairs of relatively large baselines. On the other hand, the spectral misalignment along the azimuth is very small in ERS-1/2 SLC images due to the stability of their platforms, but with SIR-C or X-SAR data it is very significant and should be performed. The over-sampling on the other hand, is computationally expensive compared to the result obtained. Anyhow, the multi-looking process absorbs most of the aliasing effects.

3.3 Flat Earth Phase Removal

At this stage the generated interferograms still contain a phase that is due to the SAR imaging geometry. The removal of this flat terrain phase is necessary so that the remaining phase values are related to the topography of the imaged terrain above the reference geometry. To achieve this, the geometric approach of determining the positions of the sensor at the slave and master orbits is used. These positions are determined by a geolocation procedure that considers the earth surface as an ellipsoid and uses the orbit state and velocity vectors available from the CEOS leader file. The respective algorithms are described by Raggam [7, 8]. The flat earth phase is computed for a number of grid points distributed over the whole quarter scene. The pixel to pixel flat earth phase is then calculated by quadratic or any higher order polynomial and then subtracted from the interferogram by a complex multiplication. But incase the sensor platform is not stable enough, such as in the SIR-C/X-SAR case, the fringe majority method can be used instead. In this method it is assumed that the maximum of the Fourier spectrum of the interferogram estimates the flat terrain phase in azimuth

and range. This phase value is then subtracted from the interferogram as a constant phase slope in the range and azimuth directions.

After the subtraction, the interferogram is then multi-looked by typically 10 pixels in azimuth and 2 pixels in range (20 look), which translates to a ground pixel resolution of about 40 by 40 meters. The multi-looked products which are usually generated from an interferogram are an amplitude image, a coherency or correlation image and a fringe image. These products are shown for a demonstration area, which is a part of the „Dortmund" test area, in figures 1, 2 and 3, respectively. Moreover, figure 4 presents a flat terrain filtered phase image of this demonstration area.

3.4 Interferogram Smoothing

The flat earth filtered interferogram image is smoothed by adaptive low pass filtering before being unwrapped. The simple moving average filter is adequate enough when the data pairs are of relatively small baseline and from flat terrain area. Otherwise, directional adaptive filters are required such as the Gaussian filter de-

Figure 1: Amplitude image of interferogram

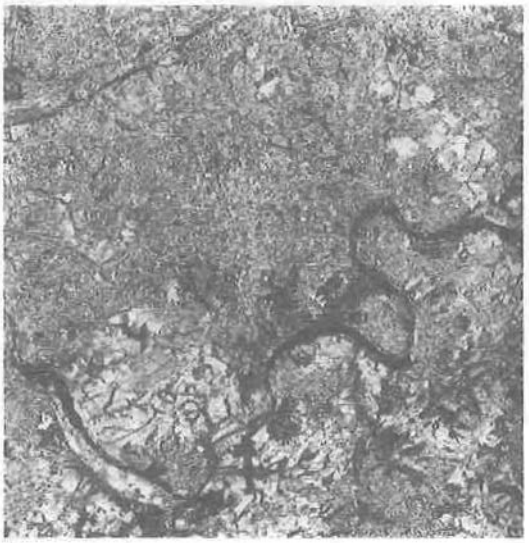

Figure 2: Coherency image

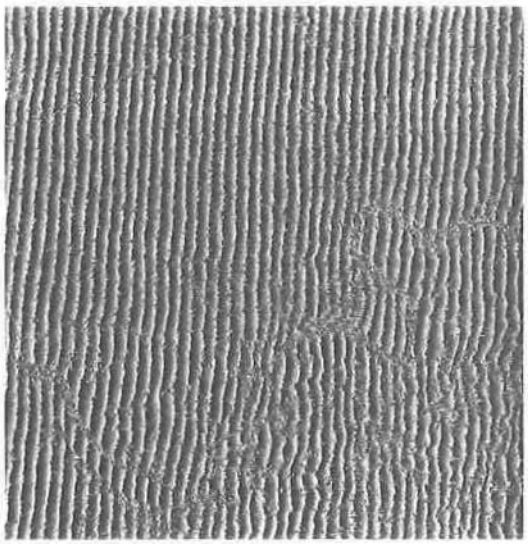

Figure 3: Fringe image

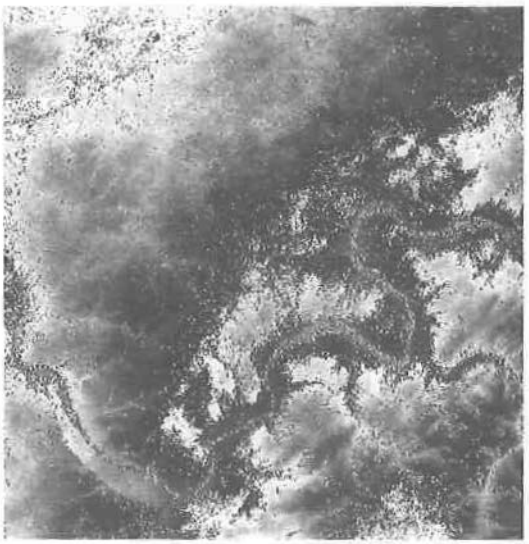

Figure 4: Flat terrain filtered fringe image

Figure 5: Smoothed fringe image

Figure 6: Unwrapped phase image

scribed by Goudtner et al. [2]. It is to be noted that experience has shown that the filter acts best when applied to the complex data or the normalised phase values. A smoothed and flat terrain filtered phase image of the demonstration area is shown in figure 5.

3.5 Phase Unwrapping

For the phase unwrapping the algorithm described by Goldstein et al. [3] was used. It first detects the difficult areas in the interferograms as residues and then connects them by placing cuts between residues of opposite signs with a condition that the total lengths of the cuts are minimised. In addition, amplitude and coherency image information were used to mask out regions showing layover and unreliable phase values. The masked pixels then aid in the cuts placing as earth lines used to discharge unpaired residues or those with long separation distance. After masking and cuts placement, the phase differences between the fringes are then integrated along paths that do not cross the cut lines or masked regions yielding the absolute phase image. This phase difference integration is frequently called phase unwrapping in the literature. The phase values of the interdicted pixels can be linearly interpolated from their unwrapped neighbours. The interpolation is just a filling procedure and does not guarantee the truthfulness of the interpolated pixel values.

In general, the unwrapped phase image already reflects the shape of the terrain, but still in the geometry of the SAR image. For the selected demonstration area, the respective product is shown in figure 6.

4. DEM Generation Procedure

The geometric imaging disposition for interferometric data is shown in figure 7. Various approaches may be used to convert the unwrapped phase values pixel-by-pixel to corresponding ground points. The procedure which has been implemented in our software is briefly described in the following.

First, the slant range difference δ_i is calculated for each pixel from the individual phase values Φ_i:

$$\delta_i = -\frac{\lambda}{4\pi} \cdot (\Phi_i + \Phi_c)$$

Usually, Φ_c is a constant phase offset. In our approach, however, linear terms in range and azimuth are additionally considered in order to compensate for converging or diverging orbits and similar effects because of erroneous a-priori information. The terms of this phase offset „function" are determined in advance by using a sufficient number of ground control points with respective reference values for δ_i and Φ_i.

Besides, the slant range distance R_1, which corrsponds to the length of vector r_1, is determined from the SAR range pixel coordinate. Then, the slant range distance R_2 and the baselength B can be calculated in a next step as follows:

$$R_2 = |\vec{r_2}| = R_1 + \delta$$
$$B = |\vec{s_2} - \vec{s_1}|$$

These entities are used to determine the angle α between baseline vector B and pointing vector $\vec{r}_1$ in sensor position $\vec{s}_1$ by the equation:

$$\cos \alpha = \frac{R_2^2 + B^2 - R_1^2}{2 \cdot B \cdot R_1}$$

Using s_1, B, α, R_1 as well as 3D vector relations, the pointing vector $\vec{r}$ and the ground point $\vec{p}$ are finally calculated.

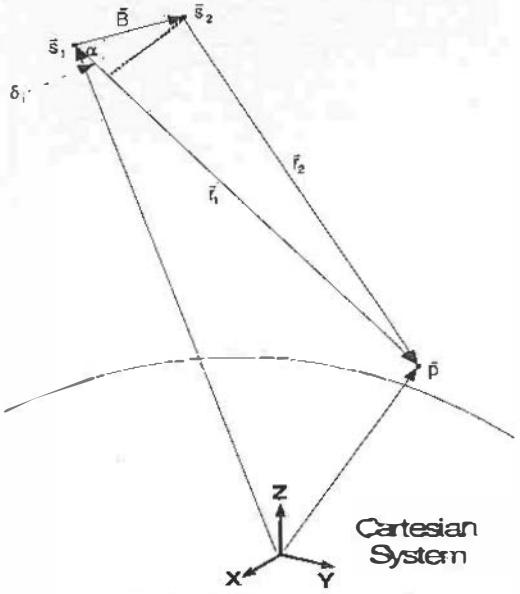

Figure 7: Geometric INSAR imaging disposition

5. DEM Generation Examples

In the following, an overview on results achieved for the individual test areas with regard to the production of digital elevation models is given.

5.1. Test area „Bonn"

The Bonn test area was subject to an investigation on the effect of atmospheric artifacts on the interferometric processing. A DEM was interferometrically produced for a part of the area covered by the ERS SLC quarter scenes. Therefore, 14 ground control points adequately distributed over the scene were measured in order to determine the phase offset induced during phase unwrapping. For comparison, a reference DEM was generated from digitised contour lines of 1 : 50000 topographic maps. From a comparison of these DEMs, deviations from the local topography with a bubble-like shape and in an extension of several hundred meters could be observed. Based on meteorological reference data, these deviations have been identified as atmospheric effects in an investigation by Kenyi et al. [4].

The INSAR generated DEM and the reference DEM for the Bonn area are shown in figures 8 and 9, respectively, in a gray value coded presentation and superimposed with contour lines. In order to assess the errors in the INSAR DEM, the height differences between the INSAR generated and the reference DEM were computed. The resulting difference DEM is shown in figure 10 in an adequate presentation. The deviations induced by the atmospheric effects are visible in the left top area of this difference DEM as dark shaded regions, corresponding to elevation errors of up to 50 meters. The overall accuracy of the INSAR derived DEM may be expressed by the standard deviation of the elevation differences, which was found to be about 11 meters.

5.2 Test area „Dortmund"

For this test area good quality interferograms could be generated from the ERS SLC data. Practically, all over the quarter scene the achieved coherency was very high except of the water bodies and some forested areas (see also figure 2). Based on ground control points measured in 1:50000 topographic maps, a DEM was generated from the unwrapped phase data. This DEM is shown in figure 11, while in figure 12 a reference DEM is presented, both being illustrated again in gray value coding and contour line superposition. Only from a comparison of the contour lines, the differences between these DEMs become obvious, whereas the pure gray value coded shapes of the terrain correspond almost perfectly. First verification activities have shown a good height correspondence for most parts of the INSAR generated DEM, with some exceptions in the hilly terrain areas. In general, it can be stated that because of the small baseline the orbits reconstruction during the DEM generation might become unstable and could lead to such local errors. Also other parameters, such as weather information, need to be investigated in order to conclude on some of these variations that have been observed in the INSAR DEM. However, to come to concrete conclusions on the verification of the INSAR DEM, further analyses are still needed. These typically could include intercomparison of INSAR DEMs of the same scene, but generated from SLC data sets of different baselines.

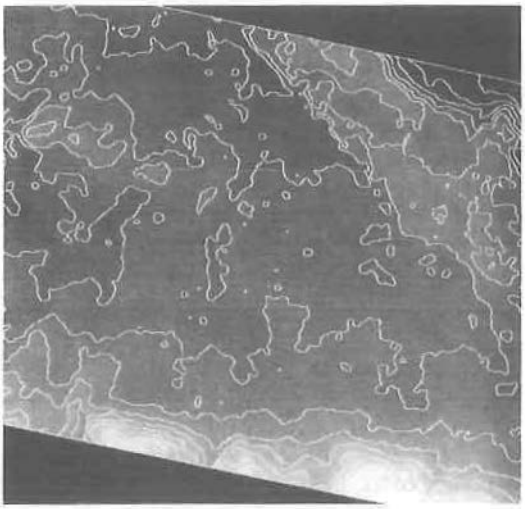

Figure 8: INSAR derived DEM for the „Bonn" test area

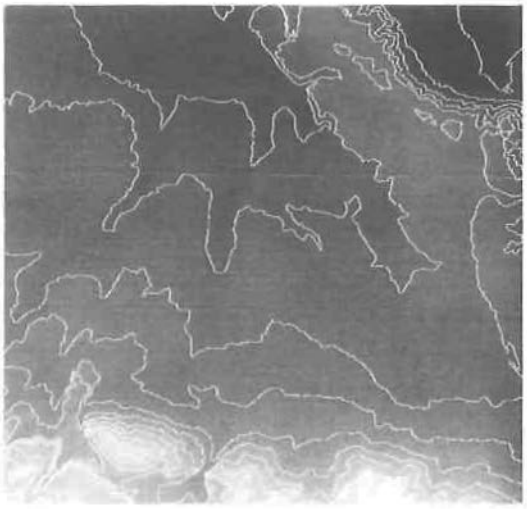

Figure 9: Reference DEM for the „Bonn" test area

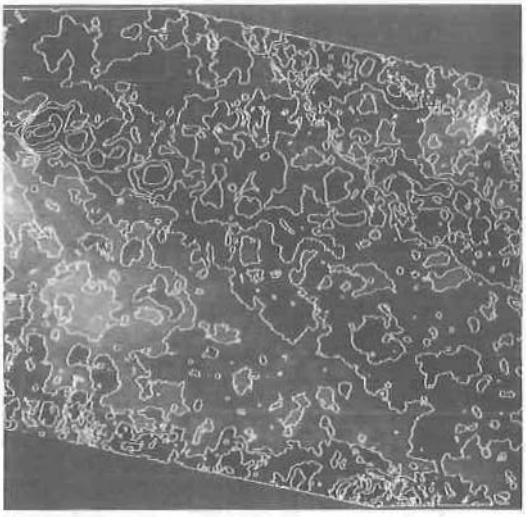

Figure 10: Difference DEM for the „Bonn" test area

5.3 Test area „Graz"

Relatively good quality interferograms were generated from the ERS-1/2 tandem data set of this test area, but coherency in some parts of the quarter scene was very low. This in particular applies to the forested areas, which by experience are rather critical for the interferometric data processing. Generally, a DEM was successfully generated from the unwrapped phase data which is shown in figure 13, while in figure 14 a reference DEM derived from topographic maps of the test area is presented. It can be noted that the INSAR derived DEM, as shown in figure 13, contains holes in some parts. In fact, these holes correspond to the areas of low coherency, where the interpolation algorithm fails to estimate reasonable values due to the wide size of these areas of unreliable phase information. Although the DEM has not been validated, it can be seen to accurately reflect the shape of the topography of the area. This can simply be deduced from the visual comparison with the map derived reference DEM in figure 14. From the initial cross checking of some points in the INSAR DEM with the reference DEM, it was observed that large deviations (about 50 m) could be found especially in the hilly regions. As mentioned before, the small baselines could be of influence in the stability of the orbits reconstruction. A comprehensive analysis, which deals with questions such as different processing chains, for example interferogram generation with and without spectral filtering, different baselines etc., is required. This could then, in our opinion, lead to good qualitative and quantitative analysis.

6. Conclusions

Interferometric processing tools have been developed and added to the RSG software being designed for the geometric processing of remote sensing image data. In general, it can be concluded that even at relatively small baselines INSAR derived DEMs give height information with acceptable errors. However, enough care must be exercised due to the fact that atmospheric turbulences can introduce errors of large magnitude in the INSAR height measure-

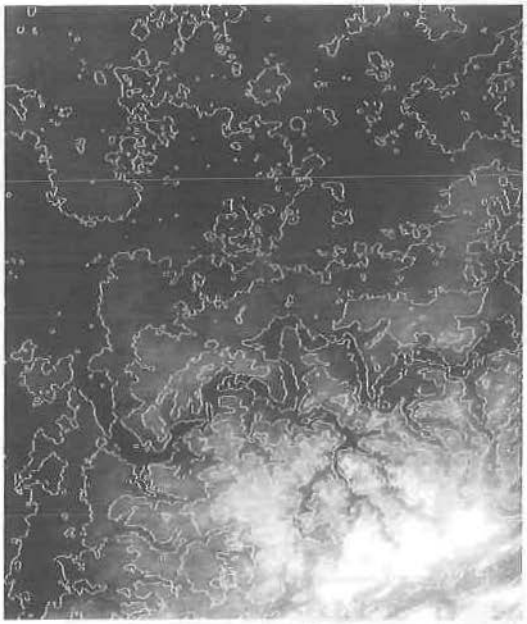

Figure 11: INSAR derived DEM for the „Dortmund" test area

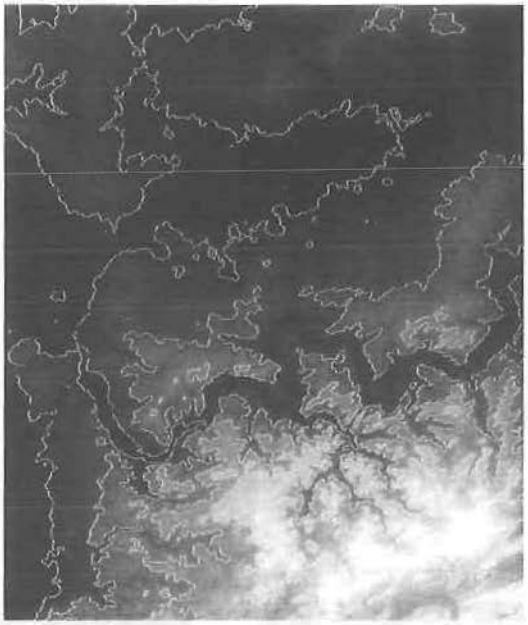

Figure 12: Reference DEM for the „Dortmund" test area

Figure 13: INSAR derived DEM for the „Graz" test area

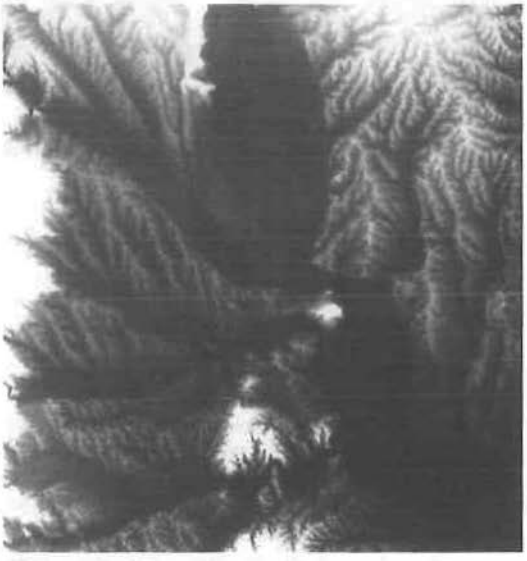

Figure 14: Reference DEM for the „Graz" test area

ments. But to come to qualitative and quantitative conclusions on the INSAR derived DEMs, further work still needs to be performed for the validation of INSAR derived DEMs. These could typically consist of SLC data sets of different baselines and from various terrain topography, different INSAR processing chains and adequate selection of control points for the DEM generation process.

Acknowledgement

The reference DEM of the Dortmund test area has been provided by the Deutsche Forschungsanstalt für Luft- und Raumfahrt (DLR) for comparative analyses. Assistance in the control point measurement and support in the production of the figures was provided by our colleagues A. Almer and S. Teufel. We thankfully acknowledge these contributions.

References

[1] *Gabriel A., Goldstein R., and Zebker H. (1989):* Mapping Small Elevation Changes Over Large Areas: Differential Ra-

dar Interferometry. J. Geophysical Research, Vol. 94, No. B7, pp. 9183–9191, July 10, 1989.

[2] *Geudtner D., Schwäbisch M., and Winter R. (1994):* SAR-Interferometry with ERS-1 Data. Proceedings of PIERS'94 Symposium, Noordwijk, The Netherlands, 11–15 July 1994.

[3] *Goldstein R., Zebker H., and Werner C. (1988):* Satellite Radar Interferometry: Two-Dimensional Phase Unwrapping. Radioscience, Vol. 23, No. 4, pp. 713–720, July–August, 1988.

[4] *Kenyi L. W., Raggam H., and Kubista E. (1996):* Feasibility of Atmospheric Effect on Interferometric Data and its Interpretation. DIBAG Report 64, ESA Contract No. 9949/92/NL/PB, JOANNEUM RESEARCH, Institute for Digital Image Processing, April 1996.

[5] *Massonnet D., Rossi M., Carmona C., Peltzer G., Feigl K., and Rabaute T. (1993):* The Displacement of Field of the Landers Earthquake Mapped by Radar Interferometry. Nature, Vol 364, No. 6433, pp. 138–142, 1993.

[6] *Prati C., Rocca F., and Monti-Guarnieri A. (1992):* SAR Interferometry Experiments with ERS-1. In Proceedings of 1st ERS-1 Symposium, Cannes, France, pp. 211–218, November 1992.

[7] *Raggam H. (1990a):* Interpolative Map-to-Image Coordinate Transformation for Spaceborne Imagery. In Proceedings of 10'th Annual IGARSS Symposium: Remote Sensing – Science for the Nineties, Vol. II, pp. 1423–1426, Washington D.C., U.S.A, May 20–24 1990.

[8] *Raggam H. (1990b):* Analytical Simulation for Quality Control of Geocoded SAR Images. Technical Note made under contract for the German PAF for ERS-1., JOANNEUM RESEARCH, Institute for Digital Image Processing, July 1990.

[9] *Zebker H., Rosen P., Goldstein R., Gabriel A., and Werner C. (1994a):* On the Derivation of Coseismic Displacement Fields Using Differential Radar Interferometry: The Landers Earthquake. J. Geophysical Research, Vol. 99, No. B10, pp. 19617–19634, 10 October 1994.

[10] *Zebker H., Werner C., Rosen P., and Hensley S. (1994b):* Accuracy of Topographic Maps Derived from ERS-1 Interferometric Radar. IEEE Trans. Geoscience and Remote Sensing, Vol. 32, No. 4, pp. 823–836, 10 October 1994.

Address of the Authors:

Dr. Lado Kenyi, Dr. Hannes Raggam, and Dr. Mathias Schardt, Institute for Digital Image Processing, Joanneum Research, Wastiangasse 6, A-8010, Graz.





Aerial photo interpretation and satellite image analysis in agricultural sciences

Werner Schneider, Renate Bartl, Hannes Burger, Joachim Steinwendner, Franz Suppan, Vienna

1. Introduction

The Universität für Bodenkultur (BOKU, University for Agricultural Sciences, Vienna) offers education and training and conducts research in the fields of agriculture, forestry, civil engineering and water management, landscape architecture and planning as well as food science and biotechnology. In most of these disciplines, data on large areas (ranging from the size of a parcel of land up to regional, national, continental or even global dimensions) are required both for scientific research and for practical operational applications. The type of information needed may concern the geometrical size, shape and location of objects, regions and phenomena on the surface of the earth (e.g. of agricultural fields or vegetation areas or areas of deforestation), it may be related to soil and vegetation properties (e.g. soil type, crop type and condition, forest damage), or it may refer to general land use patterns and landscape structures. The major advantages of using image data remotely sensed from aircraft and satellites as compared to traditional methods such as field work, statistical surveys etc. can be seen in the following points:

- quality of information: Certain information on the terrain, on the vegetation cover and on the type and distribution of objects on the terrain can be obtained much better and with higher quality from above. A bird's-eye view of forest stands yields information on the condition of tree crowns which cannot be obtained from below. The synoptic view of a landscape as represented by a satellite image allows insights into the geological, ecological and socio-economic conditions inattainable by other methods. The homogeneity of the information over large areas as offered by re-